

Singlet Oxygen Production from Singlet and Triplet States of 9,10-Dicyanoanthracene

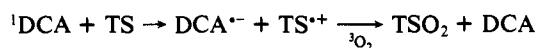
Richard C. Kanner and Christopher S. Foote*

Contribution from the Department of Chemistry and Biochemistry, University of California, Los Angeles, California 90024. Received April 1, 1991

Abstract: The mechanism and quantum yield of singlet oxygen ($^1\text{O}_2$) production by 9,10-dicyanoanthracene (DCA) has been investigated in benzene and acetonitrile; $^1\text{O}_2$ is produced from both the singlet and triplet states of DCA. Intersystem crossing enhanced by 2,5-dimethylidobenzene (DMIB) provided a direct route to ^3DCA and allowed determination of the individual contributions of ^3DCA and ^1DCA to $^1\text{O}_2$ production. Enhanced intersystem crossing can make the triplet pathway a major route under some conditions and can result in high quantum yields of $^1\text{O}_2$.

Introduction

The oxygenation of organic compounds photosensitized by dicyanoanthracene (DCA) has been extensively studied and has been shown to go by two competing mechanisms, a "Type I" electron-transfer process and a "Type II" process via singlet oxygen ($^1\text{O}_2$).^{1,2} The Type I process is exemplified by the photooxygenation of *trans*-stilbene (TS) in CH_3CN .^{3,4} In this process, singlet excited ^1DCA undergoes electron transfer from TS to form a radical cation ($\text{TS}^{+\bullet}$) and a radical anion ($\text{DCA}^{\bullet-}$). The subsequent reaction of $^3\text{O}_2$ with these radical ions gives benzaldehyde and other oxidation products.

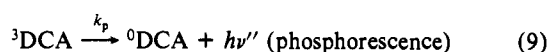
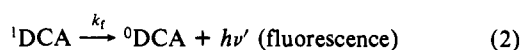


The Type II process via $^1\text{O}_2$ is exemplified by the DCA-sensitized photooxygenation of 1,2-dimethylcyclohexene, a typical olefinic $^1\text{O}_2$ substrate.⁵ In this mechanism, excited DCA is quenched by oxygen with energy transfer to form $^1\text{O}_2$, which then oxidizes 1,2-dimethylcyclohexene to give a characteristic product distribution. Rose bengal sensitized oxidation gives a very similar product distribution, and this fact and additional kinetic evidence confirmed an $^1\text{O}_2$ pathway for this substrate. Radical autoxidation gives a distinctly different product distribution. Several other alkenes gave product distributions which provided a similar "fingerprint" for $^1\text{O}_2$ in the DCA-sensitized oxygenation.⁵⁻⁸

Several possible reactions of excited DCA are shown in Scheme I. Although product distribution studies and detection of 1268-nm luminescence provided evidence for $^1\text{O}_2$ production,⁹ the intersystem crossing yield for DCA reported by Manring et al.¹⁰ was only 1.7% in CH_3CN , indicating that direct formation of triplet DCA (reaction 3) is not a major pathway for the formation of $^1\text{O}_2$ by DCA. The route to $^1\text{O}_2$ could involve direct energy transfer to $^3\text{O}_2$ from ^1DCA , either with (reaction 4) or without (reaction 7) the production of ^3DCA . An alternative is $^3\text{O}_2$ enhancement of the intersystem crossing of ^1DCA to form ^3DCA (reaction 5), which then transfers energy to oxygen (reaction 10). The first

mechanism has an overall maximum quantum efficiency for $^1\text{O}_2$ formation of 2.0 since both reactions 4 and 10 give $^1\text{O}_2$. The second and third mechanisms have maximum overall quantum efficiencies of 1.0.

Scheme I



Energy transfer from both singlet and triplet DCA to $^3\text{O}_2$ is energetically allowed. The DCA triplet energy is 41.8 kcal/mol,¹¹ which is high enough to allow exothermic transfer to $^3\text{O}_2$ to give $^1\text{O}_2$ ($^1\Delta_g$, 23 kcal/mol). Since the DCA singlet energy is 66 kcal/mol,¹¹ there is a 24.2 kcal/mol singlet-triplet energy gap, which is also large enough to excite $^3\text{O}_2$ to $^1\text{O}_2$.¹¹ Dobrowolski, Ogilby, and Foote⁹ measured the $^1\text{O}_2$ quantum yield ($\Phi_{^1\text{O}_2}$) in both C_6H_6 and CH_3CN by comparison of the 1268-nm luminescence of $^1\text{O}_2$ produced by DCA and diacenaphtho[1,2-*b*:1',2'-*b*]thiophene. The $\Phi_{^1\text{O}_2}$ of diacenaphtho[1,2-*b*:1',2'-*b*]thiophene was determined by actinometry with 2-methyl-2-pentene. They found $\Phi_{^1\text{O}_2}$ for DCA to be 2.0 in CH_3CN and 1.56 in C_6H_6 , extrapolated to infinite oxygen concentration.

However, the $^1\text{O}_2$ emission signals in this work were extremely noisy, and extrapolation led to a very large error in the quantum yield. Acridine has recently been introduced as a standard; its singlet oxygen yield has been determined by luminescence^{12,13} and

(1) Foote, C. S. In *Free Radicals in Biology*; Pryor, W. A., Ed.; Academic Press: New York, 1976; pp 85-133.

(2) Foote, C. S. *Tetrahedron* 1985, 41, 2221-2227.

(3) Eriksen, J.; Foote, C. S. *J. Am. Chem. Soc.* 1980, 102, 6083-6088.

(4) Lewis, F. D.; Bedell, A. M.; Dykstra, R. E.; Elbert, J. E.; Gould, I. R.; Farid, S. *J. Am. Chem. Soc.* 1990, 112, 8055-8064.

(5) Araki, Y.; Dobrowolski, D. C.; Goynes, T.; Hanson, D. C.; Jiang, Z. Q.; Lee, K. J.; Foote, C. S. *J. Am. Chem. Soc.* 1984, 106, 4570-4575.

(6) Cao, Y.; Zhang, B. W.; Ming, Y. F.; Chen, J. X. *J. Photochem.* 1987, 38, 131-144.

(7) Santamaria, J. *Tetrahedron Lett.* 1981, 22, 4511-4514.

(8) Steichen, D. S.; Foote, C. S. *Tetrahedron Lett.* 1979, 4363-4366.

(9) Dobrowolski, D. C.; Ogilby, P. R.; Foote, C. S. *J. Phys. Chem.* 1983, 87, 2261-2263.

(10) Manring, L. E.; Gu, C.-L.; Foote, C. S. *J. Phys. Chem.* 1983, 87, 40-44.

(11) Darmanyan, A. P. *Chem. Phys. Lett.* 1984, 110, 89-94.

(12) Gorman, A. A.; Hamblett, I.; Rodgers, M. A. J. *J. Am. Chem. Soc.* 1984, 106, 4679-4682.

Table I. Results of Plot of $\Phi_{\text{O}_2}^1$ vs $[\text{O}_2]^{-1}$ for DCA (Figure 1)

solvent	$\Phi_{\text{O}_2}^1$	corr coeff
C_6H_6	1.56 ± 0.10	1.000
CH_3CN	1.46 ± 0.10	0.999

thermal lensing,¹³ and its triplet yield is also well-documented.¹⁴ Using acridine as a standard, we have redetermined the value of $^1\text{O}_2$ production from DCA in both acetonitrile and in benzene with an improved detector. We also prepared ^3DCA directly, using enhanced intersystem crossing with 2,5-dimethyliodobenzene and determined the yield of $^1\text{O}_2$ by this path.

Experimental Section

$^1\text{O}_2$ Quantum Yields. The apparatus was a modification of the one previously described.¹⁵ DCA was excited at 355 nm using the third harmonic of a Quanta-Ray DCR-2 Nd:YAG laser. The laser pulse was filtered to remove any fundamental from the laser using a 355-nm pass/1060-nm reflecting mirror (Newport Corp.), followed with a KG-3 (Schott Glass) infrared absorbing filter. The 355-nm pulse was also filtered with a 355-nm pass/532-nm reflecting mirror. The near-infrared emission from $^1\text{O}_2$ was monitored at right angles to the laser beam and filtered with an RG-850 cutoff filter (Schott Glass) and a silicon 1100-nm cutoff filter (Infrared Optics). The detector was a 2-mm germanium diode (Opto-Electronics), with a preamplifier (OP-37, Analog Devices) operating in a transimpedance mode with a 500-K Ω feedback resistor, followed with a Comlinear CLC E220 amplifier. The signal from the detector was fed to a transient digitizer (Analogic Data 6000) where it was signal-averaged (a maximum of 16 shots) and then transferred to a PDP-11/73 for analysis. The lifetimes were determined using the Guggenheim method, and the infinity values were calculated using the Kedzay-Swinborne method.¹⁶ Quantum yields were determined by extrapolation of emission intensities to zero time as defined by the trigger pulse from a photodiode (MRD510), which monitored laser scatter from the Pellin-Brocca prism of the PHS (Prism harmonic separator) of the laser. The intensities at time zero were corrected to 100% absorption from an absorbance of 0.8 and compared to the $^1\text{O}_2$ quantum yield of acridine under air. All absorbances were measured on a Beckman 25 spectrophotometer. Various oxygen concentrations were achieved by purging the solvent with air, pure oxygen, or a 59.8:40.2 oxygen/nitrogen mixture.

Fluorescence Quenching. Fluorescence quenching experiments were performed on a SPEX Fluorolog 2 fluorimeter, exciting DCA (2.61×10^{-7} M) at 390 nm and monitoring the 434-nm fluorescence of DCA in benzene.

DCA Triplet Yield. The transient absorption spectrometer was as previously described,¹⁷ with the following modifications. The detector was an RCA IP-28 photomultiplier tube (PMT) wired in a high-current configuration. The output of the PMT was monitored across a variable-load resistor (50 Ω –100 K Ω), which could be adjusted for gain, followed by an LH0032 operational amplifier (National Semiconductor) followed by a LH0033 buffer amplifier (National Semiconductor). A bucking circuit, which applied a positive voltage in series with the output voltage across the load resistor, was used to obtain the full 6.4-V range of the digitizer. The monochromator was a 0.25 m f/3.5 Jarrell-Ash Model 82-410 with 500- μm slits. Triplet-triplet absorption of DCA was monitored at 440 nm after deoxygenation by purging with argon for 15 min. The absolute quantum yield for ^3DCA production was determined from the extinction coefficients of ^3DCA ($9000 \text{ cm}^{-1} \text{ M}^{-1}$)¹¹ and acridine ($25000 \text{ cm}^{-1} \text{ M}^{-1}$)¹⁴ at 440 nm and the value of 0.84 for Φ_{acridine}^3 , which is based upon $^1\text{O}_2$ production quantum yields using the thermal lensing technique and the reported S_{Δ} of 1.0.^{13,18}

Materials. DCA (Aldrich Chemical Co.) was recrystallized from toluene. DMIB was used as received (Lancaster Synthesis). Acridine (Aldrich) was recrystallized from toluene. All solvents were spectrograde (Mallinkrodt) or Gold Label (Aldrich).

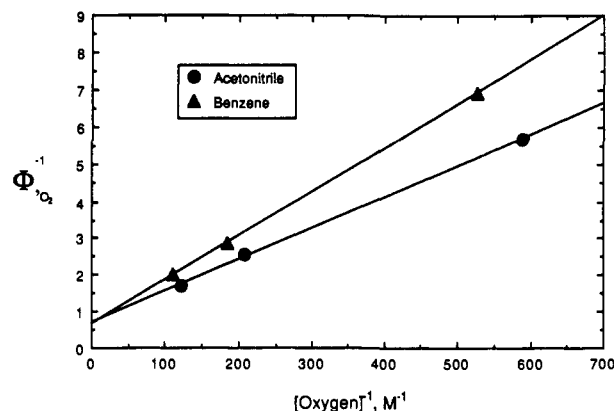


Figure 1. Plot of $\Phi_{\text{O}_2}^1$ vs $[\text{O}_2]^{-1}$ for DCA in C_6H_6 and CH_3CN . $\Phi_{\text{O}_2}^1$ was determined by reference to acridine-sensitized $^1\text{O}_2$ emission. The absorbances of DCA (2.64×10^{-4} M) and acridine (1.02×10^{-4} M) were 0.7 at 355 nm.

Results

The quantum yield for $^1\text{O}_2$ production with contributions from both ^1DCA and ^3DCA is shown in eq 1,

$$\Phi_{\text{O}_2}^1 = \frac{(k_{\text{eto}}^1 + k_{\text{sf}}^1)[^3\text{O}_2]}{k_{\text{ox}}^1[^3\text{O}_2] + \tau_{\text{DCA}}^{-1}} + \frac{(k_{\text{eto}}^1 + k_{\text{isco}})[^3\text{O}_2] + k_{\text{isc}}S_{\Delta}}{k_{\text{ox}}^1[^3\text{O}_2] + \tau_{\text{DCA}}^{-1}} S_{\Delta} \quad (1)$$

where lumped constants are defined as follows:

$$\begin{aligned} \tau_{\text{DCA}}^{-1} &= k_{\text{ic}}^1 + k_{\text{f}} + k_{\text{isc}} \\ k_{\text{ox}}^1 &= k_{\text{qo}}^1 + k_{\text{sf}}^1 + k_{\text{eto}}^1 + k_{\text{isco}} \\ k_{\text{ox}}^3 &= k_{\text{qo}}^3 + k_{\text{eto}}^3 \end{aligned}$$

As defined by Gorman et al.,¹² S_{Δ} is as follows:

$$S_{\Delta} = \frac{k_{\text{eto}}^3}{k_{\text{ox}}^3}$$

Since the direct intersystem crossing yield for DCA is very small as shown by Manning, Gu, and Foote¹⁰ (and confirmed below), $k_{\text{isc}} \ll k_{\text{eto}}^1[^3\text{O}_2]$, and eq 1 may then be rewritten in reciprocal form as follows:

$$\Phi_{\text{O}_2}^{-1} = \left(\frac{k_{\text{ox}}^1}{k_{\text{eto}}^1 + k_{\text{sf}}^1 + S_{\Delta}(k_{\text{eto}}^1 + k_{\text{isco}})} \right) + \left(\frac{\tau_{\text{DCA}}^{-1}}{k_{\text{eto}}^1 + k_{\text{sf}}^1 + S_{\Delta}(k_{\text{eto}}^1 + k_{\text{isco}})} \right) \frac{1}{[^3\text{O}_2]} \quad (2)$$

The reciprocal of the intercept of a plot of eq 2 vs $[\text{O}_2]^{-1}$ is $\Phi_{\text{O}_2}^{\infty}$, the quantum yield of singlet oxygen at infinite oxygen concentration:

$$\Phi_{\text{O}_2}^{\infty} = \frac{k_{\text{eto}}^1 + k_{\text{sf}}^1}{k_{\text{ox}}^1} + \frac{S_{\Delta}(k_{\text{eto}}^1 + k_{\text{isco}})}{k_{\text{ox}}^1}$$

In the limiting case where reaction 4 predominates, $k_{\text{eto}}^1 = k_{\text{ox}}^1$ and $S_{\Delta} = 1$, $\Phi_{\text{O}_2}^{\infty}$ is 2.0. In the other limiting case, where reaction 5 dominates ($k_{\text{eto}}^1 + k_{\text{sf}}^1 \ll k_{\text{isco}}$), $^1\text{O}_2$ is produced only from ^3DCA formed by $^3\text{O}_2$ -enhanced intersystem crossing of ^1DCA (k_{isco}). Under these conditions and where k_{isc} is small, eq 2 simplifies to eq 3.

$$\Phi_{\text{O}_2}^{-1} = \frac{k_{\text{ox}}^1}{k_{\text{eto}}^1 S_{\Delta}} + \frac{\tau_{\text{DCA}}^{-1}}{S_{\Delta} k_{\text{eto}}^1 [^3\text{O}_2]} \quad (3)$$

The reciprocal of the intercept of the plot of this equation (infinite oxygen concentration) is as follows:

$$\Phi_{\text{O}_2}^{\infty} = \frac{k_{\text{eto}}^1 S_{\Delta}}{k_{\text{ox}}^1} \quad (4)$$

(13) Redmond, R. W.; Braslavsky, S. E. *Chem. Phys. Lett.* **1988**, *148*, 523–529.

(14) Carmichael, I.; Hug, G. L. *J. Phys. Chem. Ref. Data* **1986**, *15*, 1–250.

(15) Ogilby, P. R.; Foote, C. S. *J. Am. Chem. Soc.* **1983**, *105*, 3423–3430.

(16) Moore, J. W.; Pearson, R. G. *Kinetics and Mechanism*; John Wiley & Sons: New York, 1981; pp 70–74.

(17) Spada, L. T.; Foote, C. S. *J. Am. Chem. Soc.* **1980**, *102*, 391–393.

(18) Redmond, R. W.; Braslavsky, S. E. In *Photosensitization*; NATO ASI Series H: Cell Biology; Moreno, G., Pottier, R. H., Truscott, T. G., Eds.; Springer-Verlag: Heidelberg, 1988; pp 93–95.

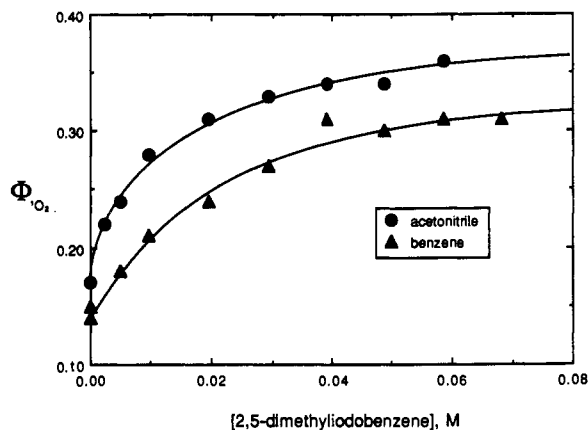
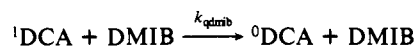
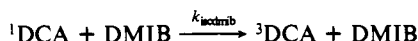


Figure 2. $^1\text{O}_2$ quantum yield ($\Phi_{^1\text{O}_2}$) versus 2,5-dimethyliodobenzene concentration in CH_3CN and C_6H_6 under air. [DCA] in acetonitrile was 1.0×10^{-4} M and in benzene was 2.56×10^{-4} M.

In the limiting case where $k_{\text{eto}}^1 = k_{\text{ox}}^1$ and $S_{\Delta} = 1$, $\Phi_{^1\text{O}_2}^{\infty}$ for this mechanism is 1.0. If $\Phi_{^1\text{O}_2}$ is greater than 1, the first mechanism is active and both singlet and triplet DCA contribute to $^1\text{O}_2$ production. If it is less than or equal to 1, either mechanism or a combination could apply. The plot of $\Phi_{^1\text{O}_2}^{-1}$ vs $[\text{DCA}]^{-1}$ is shown in Figure 1 for both C_6H_6 and CH_3CN , and the results are summarized in Table I.

$^1\text{O}_2$ Produced from ^3DCA . If S_{Δ} from ^3DCA were known, the relative contributions to $^1\text{O}_2$ production of both ^1DCA and ^3DCA could be determined. It was shown by Manring et al.¹⁰ that 2,5-dimethyliodobenzene (DMIB) enhances the intersystem crossing of DCA and allows the direct production of ^3DCA . We used this technique to measure S_{Δ} for DCA by measuring $\Phi_{^1\text{O}_2}$ as a function of DMIB concentration. Scheme II outlines mechanisms for ^3DCA production. In this scheme, k_{isdmb} is the

Scheme II



rate constant of enhanced intersystem crossing and k_{qdmib} is the rate of quenching without triplet production. From Schemes I and II, the quantum yield for $^1\text{O}_2$ production is as follows:

$$\Phi_{^1\text{O}_2} = \frac{k_{\text{eto}}^1[\text{DCA}]}{k_{\text{ox}}^1[\text{DCA}] + k_{\text{q}}[\text{DMIB}] + \tau_{^1\text{DCA}}^{-1}} + \frac{(k_{\text{eto}}^1 + k_{\text{isco}})[\text{DCA}] + k_{\text{isc}} + k_{\text{isdmb}}[\text{DMIB}]}{k_{\text{ox}}^1[\text{DCA}] + k_{\text{q}}[\text{DMIB}] + \tau_{^1\text{DCA}}^{-1}} S_{\Delta} \quad (5)$$

where $k_{\text{q}} = k_{\text{isdmb}} + k_{\text{qdmib}}$. Figure 2 is a plot of $\Phi_{^1\text{O}_2}$ versus DMIB concentration and shows that DMIB strongly enhances the production of $^1\text{O}_2$ as a result of the increased ^3DCA yield from the enhanced intersystem crossing.

Defining the following parameters,

$$F = k_{\text{ox}}^1[\text{DCA}] + k_{\text{q}}[\text{DMIB}] + \tau_{^1\text{DCA}}^{-1} \quad (6)$$

$$C = k_{\text{eto}}^1[\text{DCA}] + S_{\Delta}((k_{\text{eto}}^1 + k_{\text{isco}})[\text{DCA}] + k_{\text{isc}})$$

eq 5 can be rewritten as follows:

$$\Phi_{^1\text{O}_2} \times F = C + S_{\Delta} k_{\text{isdmb}}[\text{DMIB}] \quad (7)$$

F , the rate of decay of ^1DCA in the presence of the quenchers $^3\text{O}_2$ and DMIB, can be calculated, since the rate constants of ^1DCA fluorescence quenching by DMIB (k_{q}) and ^1DCA fluorescence quenching by $^3\text{O}_2$ (k_{ox}) and the ^1DCA fluorescence lifetime ($\tau_{^1\text{DCA}}$) are known from the literature,¹⁹ and k_{q} for DMIB in C_6H_6 is measured by standard Stern–Volmer techniques (Figure

Table II. Rate Constants for ^1DCA Fluorescence Quenching by DMIB (k_{q}) and $^3\text{O}_2$ (k_{ox}^1), and $\tau_{^1\text{DCA}}$ in CH_3CN and C_6H_6

solvent	k_{q} , s^{-1}	k_{ox}^1 , s^{-1} ^b	$\tau_{^1\text{DCA}}$, ns ^c
C_6H_6	2.82×10^9	5.0×10^9	12.4
CH_3CN	8.76×10^9 ^a	6.8×10^9	15.2

^aReference 10. ^bOgilby, personal communication. ^cReference 19.

Table III. Parameters from plot of $\Phi_{^1\text{O}_2} \times F$ vs [DMIB] (Figure 4)

solvent	$S_{\Delta} k_{\text{isdmb}}$, s^{-1}	C , s^{-1}	corr coeff
C_6H_6	$(1.12 \pm 0.01) \times 10^9$	$(1.38 \pm 0.05) \times 10^7$	0.997
CH_3CN	$(3.37 \pm 0.3) \times 10^9$	$(1.22 \pm 0.1) \times 10^7$	0.998

^a $C = k_{\text{eto}}^1[\text{DCA}] + S_{\Delta}((k_{\text{eto}}^1 + k_{\text{isco}})[\text{DCA}] + k_{\text{isc}})$.

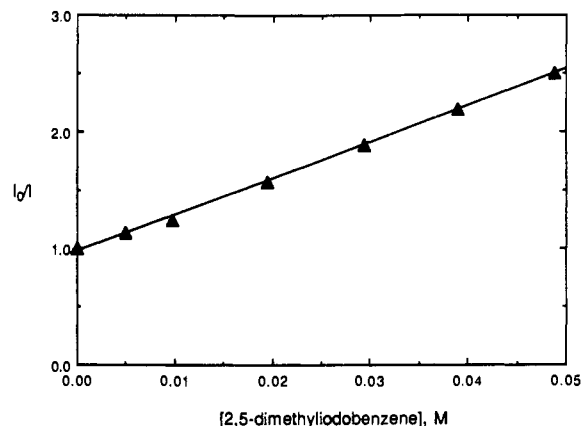


Figure 3. Stern–Volmer plot of quenching DCA (2.61×10^{-7} M) fluorescence by 2,5-dimethyliodobenzene (DMIB) in air-saturated C_6H_6 . DCA was excited at 390 nm with fluorescence monitored at 434 nm.

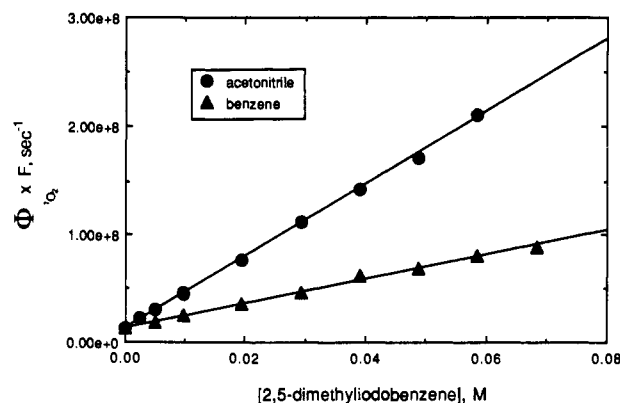


Figure 4. $^1\text{O}_2$ quantum yield ($\Phi_{^1\text{O}_2}$) $\times F$ vs 2,5-dimethyliodobenzene (DMIB) in air-saturated CH_3CN and C_6H_6 . [DCA] in CH_3CN was 1.0×10^{-4} M and in C_6H_6 was 2.56×10^{-4} M.

3). The values of these constants are listed in Table II along with the values of $\tau_{^1\text{DCA}}$.

With the rate constants from Table II, F was calculated for each data point. A plot of eq 7 for both C_6H_6 and CH_3CN is shown in Figure 4. The calculated slopes and intercepts of the plots allow calculation of the parameters in Table III.

^3DCA Yields from DMIB Determination of k_{isdmb} . In order to determine the yield of $^1\text{O}_2$ from ^3DCA , it was necessary to determine the absolute yield of ^3DCA produced by DMIB quenching of ^1DCA . This was accomplished by measuring the transient absorbance of ^3DCA at 440 nm. From the absorbance and the extinction coefficient,¹⁴ the concentration of triplet can be calculated. This was compared to the absorbance of acridine triplet¹⁴ (whose quantum yield is 0.84)¹³ under identical conditions. The singlet oxygen and triplet quantum yields are related as follows:

$$\Phi_{^1\text{O}_2} = S_{\Delta} \Phi_{\text{triplet}}$$

where S_{Δ} is defined as above¹² and Φ_{triplet} is the quantum yield

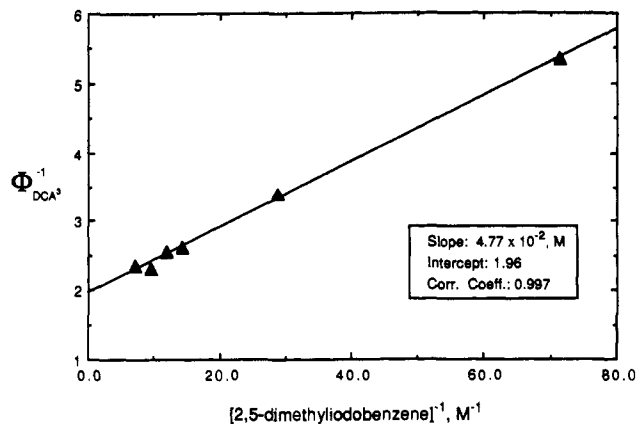


Figure 5. Plot of Φ_{DCA}^{-1} vs $[\text{DMIB}]^{-1}$ in C_6H_6 . Deoxygenated DCA ($1.2 \times 10^{-4} \text{ M}$) was excited at 355 nm.

of triplet formation. For acridine, S_{Δ} is 1.0.^{12,13} From Schemes I and II, the quantum yield for ^3DCA production in the absence of $^3\text{O}_2$ is the following:

$$\Phi_{^3\text{DCA}} = \frac{k_{\text{isc}} + k_{\text{iscdmib}}[\text{DMIB}]}{k_{\text{q}}[\text{DMIB}] + \tau_{\text{DCA}}^{-1}} \quad (8)$$

Inverting eq 8 yields:

$$\Phi_{\text{DCA}}^{-1} = \frac{k_{\text{q}}}{k_{\text{iscdmib}}} + \frac{\tau_{\text{DCA}}^{-1}}{k_{\text{iscdmib}}[\text{DMIB}]} \quad (9)$$

A plot of the data according to eq 9 is shown in Figure 5. The value of k_{iscdmib} can be calculated using values from either the slope ($k_{\text{q}}/k_{\text{iscdmib}}$) or the intercept ($\tau_{\text{DCA}}^{-1}/k_{\text{iscdmib}}$) of eq 9, since both k_{q} and τ_{DCA}^{-1} are known (Table II). The value obtained from the intercept is $1.49 \times 10^9 \text{ M}^{-1} \text{ s}^{-1}$, whereas that obtained from the slope is $1.69 \times 10^9 \text{ M}^{-1} \text{ s}^{-1}$, in good agreement.

Discussion

The value of $\Phi_{^1\text{O}_2}$ (at infinite $^3\text{O}_2$ concentration) for DCA is clearly greater than 1 (Table I) in both C_6H_6 and CH_3CN , confirming that the major pathway for production of $^1\text{O}_2$ is energy transfer from ^1DCA . Although the value in benzene agrees with that reported by Dobrowolski, Ogilby, and Foote,⁹ the value of 1.46 in CH_3CN is somewhat smaller than the 2.0 they obtained. The present results have much lower error limits since the signal-to-noise ratio of our instrument was several orders of magnitude better than that of the previous apparatus. The value of $\Phi_{^1\text{O}_2}$ determined for DNT by Dobrowolski, Ogilby, and Foote⁹ was found to be too high. Recalibrated using the acridine standard, it is 0.46 ± 0.03 in benzene and 0.39 ± 0.02 in CH_3CN , compared to values of 0.98 and 0.62, respectively.

Since the rate constant of intersystem crossing enhancement (k_{iscdmib}) is known, S_{Δ} for ^3DCA can be calculated from the values

in Table III to be 0.70 ± 0.20 in benzene (error in extinction coefficient of ^3DCA absorption reported by Darmanyan¹¹). The expression for $\Phi_{^1\text{O}_2}$ can be written:

$$\Phi_{^1\text{O}_2} = \Phi_{\text{singlet}} + \Phi_{\text{triplet}}S_{\Delta} \quad (10)$$

where Φ_{singlet} (the yield of $^1\text{O}_2$ by direct quenching of ^1DCA) and Φ_{triplet} (the yield of ^3DCA via all routes) are given by eqs 11 and 12, respectively.

$$\Phi_{\text{singlet}} = \frac{(k_{\text{eto}}^{-1} + k_{\text{sf}}^{-1})[^3\text{O}_2]}{k_{\text{ox}}^{-1}[^3\text{O}_2] + \tau_{\text{DCA}}^{-1}} \quad (11)$$

$$\Phi_{\text{triplet}} = \frac{(k_{\text{eto}}^{-1} + k_{\text{isco}}^{-1})[^3\text{O}_2]}{k_{\text{ox}}^{-1}[^3\text{O}_2] + \tau_{\text{DCA}}^{-1}} \quad (12)$$

Since S_{Δ} in benzene is 0.7, the maximum value of singlet O_2 quantum yield possible would be 1.7. Since $\Phi_{^1\text{O}_2}$ at infinite O_2 is 1.56, it is clear that any contributions from k_{sf}^{-1} and k_{isco}^{-1} must be very small, although they cannot be determined exactly. Thus, by far the predominant route to singlet oxygen comes from the double energy-transfer pathway in benzene. If the other pathways are actually zero, the quantum yield of singlet oxygen production from quenching ^1DCA is 0.86. Although S_{Δ} in CH_3CN is not known, the value of $S_{\Delta}k_{\text{iscdmib}}$ (3.37×10^9 : 1.12×10^9), obtained from eq 7 for both CH_3CN and C_6H_6 , is 3.0, the same as the value of k_{q} (the total rate of ^1DCA quenching by DMIB) for the two solvents, suggesting that S_{Δ} is the same in the two solvents. Using this assumption, the quantum yield of singlet oxygen production from quenching ^1DCA in CH_3CN is 0.76.

From the intercept of eq 9, the efficiency of ^3DCA production by DMIB enhancement is 50%. This value implies that the value Manring, Gu, and Foote¹⁰ determined for the natural intersystem crossing yield is too high by a factor of 2 since they assumed that DMIB quenches ^1DCA to yield ^3DCA with 100% efficiency. The quantum yield of natural intersystem crossing in DCA is therefore reduced from 1.7% to 0.85%. This low value, along with the low extinction coefficient ($9000 \text{ cm}^{-1} \text{ M}^{-1}$),¹¹ explains why we could not detect ^3DCA absorption in the absence of intersystem crossing enhancers.

These results indicate that $^3\text{O}_2$ quenching of ^1DCA is essentially the only route to the production of $^1\text{O}_2$ by DCA and that quenchers of ^1DCA should decrease $^1\text{O}_2$ production unless they produce ^3DCA . This conclusion is tested for the *trans*-stilbene/DCA system in the accompanying paper.²⁰

Acknowledgment. Supported by NSF Grant Nos. CHE89-11916 and CHE86-11873 and NIH GM-20081.

Registry No. DCA, 1217-45-4; O_2 , 7782-44-7; 1-iodo-2,5-dimethylbenzene, 1122-42-5.

(20) Kanner, R. C.; Foote, C. S. *J. Am. Chem. Soc.*, following paper in this issue.